Functional Redundancy of AtFtsH Metalloproteases in Thylakoid Membrane Complexes[1]

Fei Yu, Sungsoon Park, and Steven R. Rodermel*

Department of Genetics, Development, and Cell Biology, Iowa State University, Ames, Iowa 50011

FtsH is an ATP-dependent metalloprotease found in bacteria, mitochondria, and plastids. Arabidopsis (*Arabidopsis thaliana*) contains 12 AtFtsH proteins, three in the mitochondrion and nine in the chloroplast. Four of the chloroplast FtsH proteins are encoded by paired members of closely related genes (*AtFtsH1* and *5*, and *AtFtsH2* and *8*). We have previously reported that AtFtsH2 and 8 are interchangeable components of AtFtsH complexes in the thylakoid membrane. In this article, we show that the *var1* variegation mutant, which is defective in *AtFtsH5*, has a coordinate reduction in the AtFtsH2 and 8 pair, and that the levels of both pairs are restored to normal in *var1* plants that overexpress *AtFtsH1*. Overexpression of *AtFtsH1*, but not *AtFtsH2/VAR2*, normalizes the pattern of *var1* variegation, restoring a nonvariegated phenotype. We conclude that AtFtsH proteins within a pair, but not between pairs, are interchangeable and functionally redundant, at least in part. We further propose that the abundance of each pair is matched with that of the other pair, with excess subunits being turned over. The variegation phenotype of *var1* (as well as *var2*, which is defective in AtFtsH2) suggests that a threshold concentration of subunits is required for normal chloroplast function. *AtFtsH1*, *2*, *5*, and *8* do not show evidence of tissue or developmental specific expression. Phylogenetic analyses revealed that rice (*Oryza sativa*) and Arabidopsis share a conserved core of seven FtsH subunit genes, including the *AtFtsH1* and *5* and *AtFtsH2* and *8* pairs, and that the structure of the present-day gene families can be explained by duplication events in each species following the monocot/dicot divergence.

FtsH is an ATP-dependent metalloprotease that is ubiquitous among prokaryotes and eukaryotes (Beyer, 1997). It is named for the distinctive *filamentation temperature sensitive* phenotype that a mutation in the gene for FtsH causes in *Escherichia coli* (Suzuki et al., 1997). Among prokaryotic and eukaryotic photosynthetic organisms, *FtsH* genes are members of multigene families. There are 12 members of this family in Arabidopsis (*Arabidopsis thaliana*; *AtFtsH* genes), nine of which are targeted to the chloroplast (AtFtsH1, 2, 5, 6, 7, 8, 9, 11, 12) and three to the mitochondrion (AtFtsH3, 4, 10; Lindahl et al., 1996; Chen et al., 2000; Sakamoto et al., 2003; Yu et al., 2004). Eight of the 12 proteins comprise four pairs of highly homologous enzymes (Sakamoto et al., 2003; Yu et al., 2004). These homologs likely arose by duplication events that occurred during the evolution of the Arabidopsis genome (Vision et al., 2000). The organization of monocot *FtsH* gene families has not been reported.

Reverse and forward genetics experiments have revealed that most *AtFtsH* mutants do not have readily visible phenotypes (Sakamoto et al., 2003; F. Yu and S. Rodermel, unpublished data). Notable exceptions include the *var1* and *var2* variegation mutants of Arabidopsis (Martínez-Zapater, 1993; Chen et al., 1999, 2000; Takechi et al., 2000; Rodermel, 2001; Sakamoto et al., 2002). Whereas cells in the green leaf sectors of these mutants contain morphologically normal chloroplasts, cells in the white sectors contain vacuolated plastids lacking organized lamellae. At least in the case of *var2*, the white sectors are heteroplastidic and contain rare, normal-appearing chloroplasts in addition to the white plastids (Chen et al., 1999). This plastid autonomy suggests that plastids do not respond similarly in the mutant background. The distinctive phenotypes of *var1* and *var2* permitted the cloning of the responsible genes, namely, *AtFtsH5* and *AtFtsH2*, respectively (Chen et al., 2000; Takechi et al., 2000; Sakamoto et al., 2002). Because *var1* and *var2* have uniform genetic constitutions, a major question is how cells in the green sectors are able to bypass the requirement for AtFtsH5 (in the case of *var1*) or AtFtsH2 (in the case of *var2*) during the process of chloroplast biogenesis.

One consequence of the dearth of *AtFtsH* mutants is that little is known about the functions of FtsH in higher plants. FtsH-like proteins have been implicated in the degradation of unassembled cytochrome b_6f Rieske FeS proteins in the thylakoid membrane (Ostersetzer and Adam, 1997). The first identified activity of FtsH came from in vitro studies in the Adam group showing that AtFtsH1 is involved in the D1 repair cycle of PSII, where it catalyzes the proteolytic degradation of photodamaged D1 proteins (Lindahl et al., 2000). AtFtsH2 and 5 also appear to be involved in photoprotection, inasmuch as *var2* and *var1* are more sensitive than wild type to PSII photoinhibition, and D1 degradation is slowed in *var2*

(Bailey et al., 2002; Sakamoto et al., 2002). AtFtsH2 might also be involved in membrane fusion and/or translocation events since it bears high similarity to the pepper Pftf (plastid fusion and/or translocation factor) protein (Hugueney et al., 1995; Chen et al., 2000).

AtFtsH is present in multimeric complexes in plastid membranes (Sakamoto et al., 2003; Yu et al., 2004). These appear to be heteromeric and homomeric in nature. To better characterize these complexes, we reported that two AtFtsH-containing bands migrate near one another on two-dimensional (2-D) green gels of Arabidopsis thylakoid membranes (Yu et al., 2004). These bands contain the products of two of the three plastid *AtFtsH* gene pairs—an upper band (containing AtFtsH1 and 5) and a lower band (containing AtFtsH2 and 8). We observed that both bands are decreased in amount in *var2* and, further, that the levels of these bands are restored to normal in transgenic *var2* that overexpresses *AtFtsH8*. Overexpression of *AtFtsH8* also rescues the variegation phenotype of *var2*, indicating that AtFtsH2 and 8 are functionally redundant, at least in part. Consistent with this notion, both genes have similar expression patterns, being abundantly expressed in photosynthetic tissues (Yu et al., 2004).

Based on these data, we suggested a model in which AtFtsH2 and 8 are functionally interchangeable and are capable of stabilizing AtFtsH1 and 5 in the thylakoid membrane (Yu et al., 2004). In support of this model, Sakamoto et al. (2003) demonstrated via coimmunoprecipitation that members of each pair might interact, although the precise interactions could not be determined because the polyclonal antibodies that were used detect both members of each pair (Sakamoto et al., 2003). The purpose of this investigation was to test elements of our model. First, we wanted to assess the functional relatedness of AtFtsH1 and AtFtsH5. Are they interchangeable? Do they have similar expression patterns? Second, we wanted to test whether members of the AtFtsH2 and 8 pair are interchangeable with members of the AtFtsH1 and 5 pair. Finally, we wanted to take advantage of the nearly complete genome sequence of rice (*Oryza sativa*) to ask whether the two AtFtsH pairs are unique to Arabidopsis or whether they have a broader significance in FtsH complex formation.

RESULTS

Interchangeability of Subunits in the Upper AtFtsH-Containing Band

AtFtsH1 and *AtFtsH5* are the most closely related members of the *AtFtsH* gene family in Arabidopsis (approximately 90% amino acid identity). Based on our previous results showing that members of another closely related *AtFtsH* gene pair—*AtFtsH2* and *AtFtsH8*—have redundant functions, we wanted to examine whether the same is true for *AtFtsH1* and *AtFtsH5*. To test this hypothesis, we overexpressed

AtFtsH1 in the *var1-1* variegation mutant, which defines the *AtFtsH5* locus (Fig. 1A; Sakamoto et al., 2002). The *var1-1* allele has a nucleotide insertion in its N terminus that is predicted to generate an early stop codon; if stable, a truncated translation product would be produced lacking most of the functional domains of the protein. Taken together with the finding that *AtFtsH5* mRNAs are not detectable, this suggests that *var1-1* is likely a null allele (Sakamoto et al., 2002).

Figure 1A shows the results of the overexpression experiments. Full-length *AtFtsH1* cDNAs were amplified by reverse transcription (RT)-PCR, cloned into a binary vector under the control of the cauliflower mosaic virus (CaMV) 35S promoter, and transformed into *var1-1* via Agrobacterium-mediated transformation. A number of kanamycin-resistant lines were identified in the T1 generation; all resembled wild-type plants. A representative line, designated C5W1No2, was selected for further study (Fig. 1A). Southern-blot analysis revealed that this line contains a single T-DNA insertion (Fig. 1B). This is in accord with genetic data showing that selfing of C5W1No2
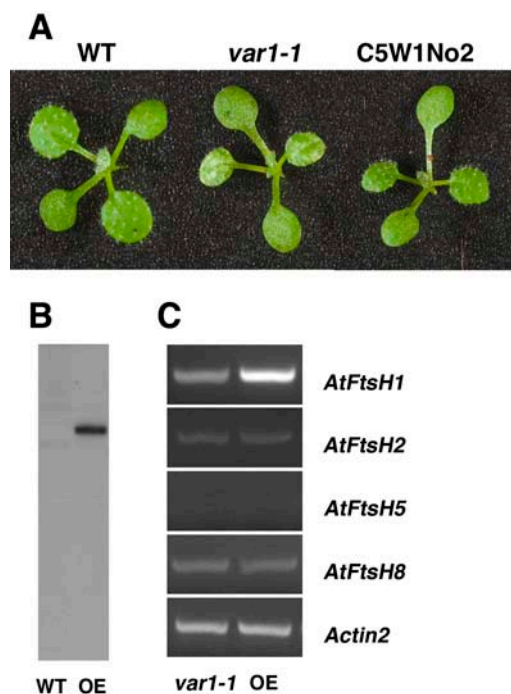

Figure 1. Complementation of *var1-1* by overexpression of *AtFtsH1*. A, Phenotypes of wild type, *var1-1*, and *var1-1* transformed with an *AtFtsH1* cDNA under the control of the CaMV 35S promoter (C5W1No2). A T2 generation C5W1No2 plant is shown. All the plants were 10 d old. B, Southern-blot of wild type and C5W1No2. OE, Overexpression. Genomic DNAs from wild type and C5W1No2 were digested with *Hin*dIII, and the Southern-blot was probed with ^{32}P-labeled *NPTII* sequences. C, Total cell RNAs were isolated from the green sectors of *var1-1* and from leaves of C5W1No2 (OE). RNA amounts were determined by semiquantitative RT-PCR as described in "Materials and Methods." The RT-PCR products were electrophoresed through 1.5% agarose gels and stained with ethidium bromide. *Actin2* served as a control.

gives rise to green and variegated T2 progeny in a ratio of approximately 3:1 (data not shown). Green T2 progeny were used in the experiments described below.

Whereas the data in Figure 1A are consistent with the idea that overexpression of *AtFtsH1* rescues the variegation phenotype of *var1-1*, it was necessary to confirm this at the level of *AtFtsH1* expression. Semiquantitative RT-PCR analyses (Fig. 1C) revealed that the transcript levels of *AtFtsH1* are sharply elevated in C5W1No2 compared to *var1-1*. By contrast, *AtFtsH2* and *AtFtsH8* mRNA levels are normal in the overexpressor. Only trace amounts of the *AtFtsH5* transcript are present in *var1-1* (as anticipated from Sakamoto et al., 2002) and C5W1No2.

To examine protein accumulation in the overexpression plants, we performed 2-D green gel analyses of Arabidopsis thylakoid membrane proteins. Previous studies have shown that two AtFtsH-containing bands can be resolved on green gels of Arabidopsis thylakoids: upper and lower bands consisting, respectively, of AtFtsH1 and 5 and AtFtsH2 and 8 (Yu et al., 2004). Whereas both AtFtsH-containing bands are reduced in abundance in *var1-1* (Fig. 2A), they are restored to normal in C5W1No2 (Fig. 2B). To confirm this finding, we performed western-immunoblot analyses on thylakoid membrane proteins fractionated by one-dimensional SDS-PAGE. To detect AtFtsH1 specifically, we generated an antibody against a peptide that is unique to this protein (see "Materials and Methods"). This antibody reacts with AtFtsH1 proteins that are expressed in *E. coli*, but not with *E. coli*-expressed AtFtsH5 or AtFtsH2 (data not shown). We detected similar levels of AtFtsH1 in wild type and *var1-1*, but a significant increase in C5W1No2 (Fig. 2C). Western immunoblots were also probed with an antibody that detects both AtFtsH2 and 8 (Yu et al., 2004). As illustrated in Figure 2D, the band containing AtFtsH2 and 8 is decreased in amount in *var1-1*, but is present at normal levels in C5W1No2. In summary, the data in Figure 2, A to C, are consistent with the idea that (1) wild-type AtFtsH complexes contain optimal levels of the 1-5 and 2-8 pairs; (2) *var1-1* has a reduction in 5, but not 1, and this is matched by a reduction in 2 and 8; and (3) optimal complex levels (as found in the wild type) can form when 1 is overexpressed in *var1-1*; these complexes contain 1 and 2-8.

Examination of the patterns of protein expression on the 2-D green gels revealed that, with the exception of the AtFtsH-containing bands, there were no significant differences in protein accumulation among the overexpression, wild-type, and *var1-1* plants (data not shown). To verify this conclusion, we generated polyclonal antibodies to representative thylakoid proteins, including the D1 protein of PSII, cytochrome b_6f Rieske protein (PetC), and the α-subunit of the plastid membrane ATP synthase. Figure 2D shows that the steady-state levels of all three proteins are similar in the three plants. This suggests that an alteration in AtFtsH protein abundance does not have major pleiotropic effects, at least in the green leaf sectors of the mutants.
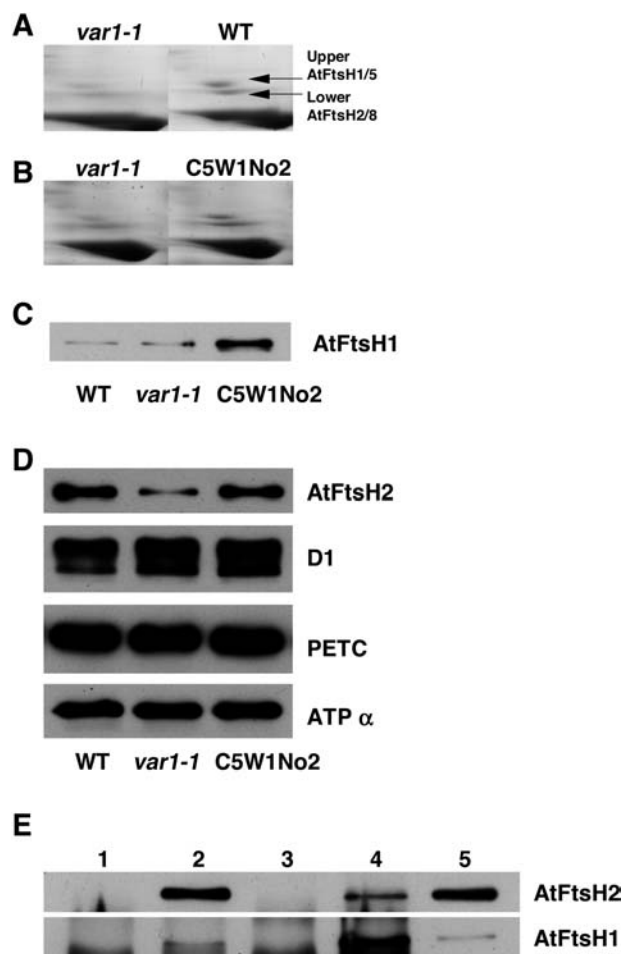

Figure 2. Two-dimensional green gel and western-immunoblot analyses. A and B, Comparison of the upper and lower AtFtsH-containing bands of *var1-1* and wild type (A) and *var1-1* and C5W1No2 (B). Thylakoid membranes corresponding to equal amounts of chlorophyll were loaded on the native gels. C, Western immunoblots of wild type, *var1-1*, and C5W1No2 thylakoid membranes. Thylakoid membranes corresponding to 2.5 μg of chlorophyll were loaded in each lane of a denaturing, 12% SDS-polyacrylamide gel. Membranes were incubated with polyclonal antibodies specific for AtFtsH1. D, Western immunoblots of wild type, *var1-1*, and C5W1No2 thylakoid membranes. Nitrocellulose filters were incubated with polyclonal antibodies to AtFtsH2/VAR2, the D1 protein of PSII, the PetC (Rieske) protein of the cytocrome b_6f complex, and the α-subunit of the proton-translocating ATP synthase. Protein loadings were the same as in Figure 2C. E, Coimmunoprecipitation of AtFtsH1 and AtFtsH2 and 8. Immunoprecipitates were resolved by SDS-PAGE and immunoblots were probed with AtFtsH1 and VAR2 antibodies. Shown are immunoprecipitated samples from VAR2 preimmune serum (lane 1), VAR2 antibody (lane 2), AtFtsH1 preimmune serum (lane 3), and AtFtsH1 antibody (lane 4). Each lane represents a thylakoid membrane corresponding to approximately 10 μg of chlorophyll. Lane 5 is a thylakoid membrane control corresponding to 5 μg of chlorophyll.

Using polyclonal AtFtsH5/VAR1 and AtFtsH2/VAR2 antibodies, it was reported that VAR1 and VAR2 might interact directly (Sakamoto et al., 2003). One factor complicating these studies was the lack of isoform-specific antibodies, i.e. their AtFtsH5/VAR1

antibody detected 1 and 5, and their AtFtsH2/VAR2 antibody detected 2 and 8. With the availability of AtFtsH1-specific antibodies, we wanted to test whether 1 interacts with the 2-8 pair, as suggested in our model of AtFtsH complex formation (Yu et al., 2004). In these experiments, we coimmunoprecipitated thylakoid membrane samples from wild-type Columbia using our AtFtsH1 or AtFtsH2/VAR2 antibodies; the latter antibodies, as mentioned earlier, detect 2 and 8. Figure 2E (lane 5) shows a western immunoblot of control thylakoid membranes: Bands corresponding to 2 and 8 (top) and 1 (bottom) can be seen. The relatively low abundance of AtFtsH1 in the membranes of wild type confirms the data in Figure 2C. In lane 4, the AtFtsH1 antibody was used to coimmunoprecitate thylakoid proteins. The immunoprecipitates were then electrophoresed on polyacrylamide gels and subjected to western analysis, using either the VAR2 or AtFtsH1 antibodies as probes. Bands containing 1 and 2 and 8 are visible, suggesting that 1 interacts with 2 and/or 8. In complementary experiments, the VAR2 antibody was used to coimmunoprecipitate thylakoid proteins (lane 2). Again, bands corresponding to 1 and 2 and 8 were observed on the western blots. This confirms the data in lane 4. As expected, coimmunoprecitation with preimmune sera did not give rise to bands on the western blots (lanes 1 and 3). We conclude that 1 interacts with 2 and/or 8 in AtFtsH complexes in the thylakoid.

Considered together, the data in Figures 1 and 2 show that AtFtsH1 overexpression rescues the *var1-1* variegation phenotype. This suggests that AtFtsH1 and 5 are interchangeable in thylakoid membranes. The data also show that there are coordinate changes in the levels of the proteins in the upper and lower bands in wild type, *var1-1*, and the overexpression plants. Control of subunit abundance likely occurs posttranscriptionally, since the overexpression plants have normal levels of *AtFtsH2* and *8* mRNAs, but reduced amounts of AtFtsH2 and 8 proteins. Perhaps the simplest hypothesis is that AtFtsH1 is interchangeable with AtFtsH5 in AtFtsH complexes, and that AtFtsH1 exerts its effect by stabilizing AtFtsH2 and 8 in the membrane.

One prediction of the above hypothesis is that down-regulation of AtFtsH1 protein levels in a *var1-1* background should result in plants with a more severe phenotype than *var1-1*. A complete lack of AtFtsH1 and 5 might be lethal if these proteins are essential for viability. To test this, we transformed *var1-1* with an antisense *AtFtsH1* cDNA driven by the CaMV 35S promoter. A number of antibiotic-resistant T1 lines were selected and selfed. Figure 3 shows the T2 progeny from a representative T1 line. These plants have a variety of color phenotypes that range from variegations similar to *var1-1* (Fig. 3A) to partially albino (Fig. 3, B–D) and completely albino (Fig. 3, E and F). PCR was used to confirm the presence of the antisense construct in the individual T2 plants (data not shown). However, we did not try to monitor changes in
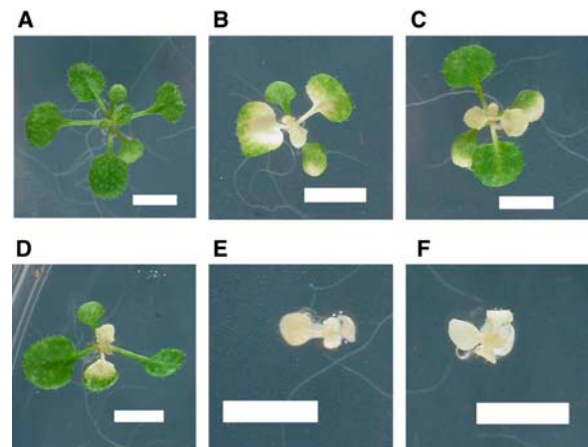

Figure 3. Antisense down-regulation of *AtFtsH1* expression in *var1-1*. A partial *AtFtsH1* cDNA was cloned in reverse orientation behind the CaMV 35S promoter, and the construct was transformed into *var1-1*. Representative T2 plants from an antibiotic-resistant T1 plant are shown. These plants have a range of color phenotypes, from those that are similar to *var1-1* (A) to those that are partially albino (B–D) or completely albino (E and F). This variability was observed in the T2 progeny of multiple independent T1 lines. Bars = 5 mm.

AtFtsH1 expression in these plants because the parental *var1-1* mutants have extremely low levels of AtFtsH1 mRNAs and proteins (see Figs. 1C and 2C). Nonetheless, the phenotypes of the antisense mutants are consistent with the idea that down-regulation of AtFtsH1 in a background that lacks AtFtsH5 can be lethal.

Expression of *AtFtsH1* and *AtFtsH5*

To examine *AtFtsH1* and *AtFtsH5* expression, we generated transgenic Columbia plants that express *AtFtsH1* promoter-GUS and *AtFtsH5* promoter-GUS fusions. Figure 4 shows that GUS activities are similar in seedlings (Fig. 4, A and C) and fully expanded older leaves in both sets of transformants (Fig. 4, B and D). Examination of other growth stages did not reveal obvious staining differences between the two constructs (data not shown). We conclude that *AtFtsH1* and *AtFtsH5* promoter activities are similar to one another, and that these genes are ubiquitously expressed, especially in green organs of the plants. These expression patterns resemble those of *AtFtsH2* and *AtFtsH8*, as previously reported (Yu et al., 2004).

Interchangeability of Subunits between the Upper and Lower AtFtsH-Containing Bands

Considered together with previous results (Sakamoto et al., 2003; Yu et al., 2004), the current data suggest that AtFtsH forms multimeric complexes in thylakoid membranes, and that these complexes contain at least two pairs of interchangeable subunits: AtFtsH2 and 8 (lower band) and AtFtsH1 and 5 (upper band). The question arises as to whether FtsH homologs in different pairs are interchangeable. To address this
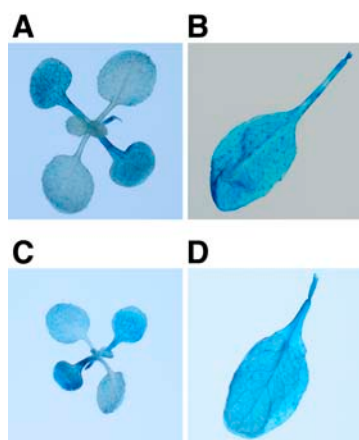
Figure 4. *AtFtsH1* and *AtFtsH5/VAR1* expression. Constructs containing promoter-GUS fusions were generated and transformed into wild type (Columbia). GUS activities were visualized by histochemical staining of fusions with the *AtFtsH1* promoter (A and B) and the *AtFtsH5/VAR1* promoter (C and D). Illustrated are 10-d-old green seedlings (A and C) and fully expanded leaves from 20-d-old plants (B and D).

question, we tested whether overexpression of *AtFtsH2* can rescue the *var1* variegation phenotype, i.e. whether AtFtsH2 can substitute for AtFtsH5. For these experiments, we generated a construct in which the full-length *AtFtsH2* cDNA was placed under the control of the CaMV 35S promoter, then transformed into *var1-1*. As a control, the construct was transformed into the *var2-4* variegation mutant, which lacks AtFtsH2. Figure 5, B and D, shows that *AtFtsH2* transcripts are significantly elevated in both sets of transformed plants. Yet, *AtFtsH2* overexpression is only able to rescue the *var2-4* variegation (Fig. 5A). A failure to rescue the *var1-1* variegation was observed in multiple lines (Fig. 5C).

Despite the sharply increased levels of *AtFtsH2/VAR2* mRNAs in the C5W2 plants, AtFtsH2 and 8 protein levels are the same in these plants as in *var1-1*, i.e. excess AtFtsH2 does not accumulate (Fig. 5E). AtFtsH1 protein levels are also similar in the two sets of plants. Perhaps the simplest hypothesis is that AtFtsH2 cannot substitute for AtFtsH5. If so, we hypothesize that *AtFtsH2* mRNAs are translated in *var1-1*, since they appear to be translatable in *var2-4*, but that AtFtsH2 proteins are turned over posttranslationally because there are not enough compatible partners (AtFtsH1 in *var1-1*) to form stable complexes.

OsFtsH Gene Family in Rice

At least three different efforts are under way to sequence the rice genome (about 420 megabases in size), and draft sequences have been published from the *japonica* cultivar (approximately 389 megabases; Goff et al., 2002) and from the *indica* cultivar (approximately 361 megabases; Yu et al., 2002). In addition, The Institute for Genomic Research (TIGR) has recently released its third version (December 30, 2004) of

annotations of pseudomolecules (virtual contigs) from the International Rice Genome Sequencing Project (IRGSP; http://rgp.dna.affrc.go.jp/IRGSP/index.html), encompassing approximately 370 megabases of the genome. This resource is easy to access (http://www.tigr.org/tdb/e2k1/osa1). To determine the *FtsH*
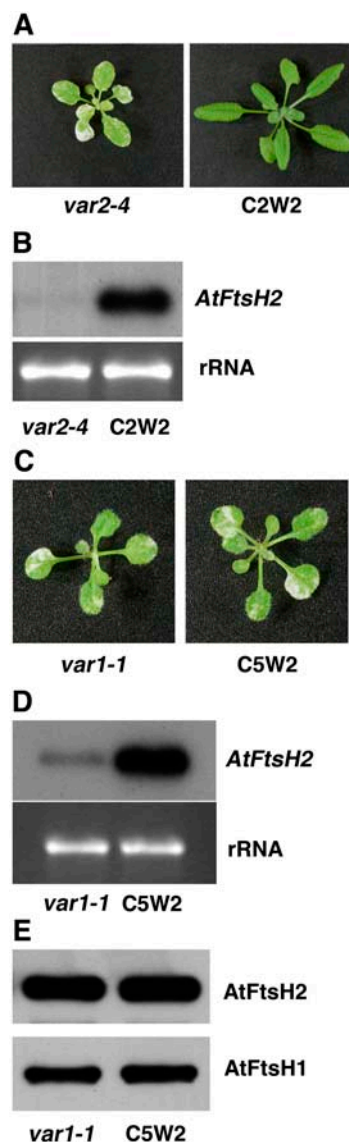

Figure 5. Overexpression of *AtFtsH2/VAR2* in *var2-4*. A, A construct containing a full-length *AtFtsH2/VAR2* cDNA driven by the CaMV 35S promoter was transformed into *var2-4*. C2W2 is a representative T2 plant. B, Total cell RNAs were isolated from *var2-4* and C2W2, and northern-blot analysis was performed using 2 μg of RNA per gel lane; the blot was probed with ^{32}P-labeled *AtFtsH2/VAR2* cDNA. Ethidium bromide-staining of the 18S RNA band on the agarose gel is shown as a loading control. C, The same construct was transformed into *var1-1*. C5W2 is a representative T2 plant. D, Total cell RNAs were isolated from *var1-1* and C5W2, and northern-blot analysis was performed as described in B. E, Steady levels of AtFtsH2/VAR2 and AtFtsH1 in *var1-1* and C5W2 thylakoid membranes were compared by western-immunoblot analysis. Thylakoid membranes corresponding to 5 μg of chlorophyll were loaded in each lane.

gene complement in rice (*OsFtsH* genes), we searched the annotated pseudomolecule database and identified a total of nine FtsH homologs, designated *OsFtsH1* through *OsFtsH9* (Table I). All nine appear to be expressed insofar as each is represented in the databases by cDNAs and expressed sequence tags (ESTs).

Figure 6 shows the phylogenetic relatedness of the nine *OsFtsH* genes compared to the 12 Arabidopsis *AtFtsH* genes and four Synechocystis *FtsH* genes that are present in the fully sequenced genomes of the latter two organisms. Full-length protein sequences were used in the analyses. Several features can be discerned. First, for every Arabidopsis *AtFtsH* gene (or closely related gene pair), there is a corresponding gene (or gene pair) in rice, except for *AtFtsH12*. Second, there are four closely related Arabidopsis gene pairs—*AtFtsH1/5*, *AtFtsH2/8*, *AtFtsH3/10*, and *AtFtsH7/9*—of which three are localized in plastids and one in the mitochondrion. The only conserved pair is the mitochondrial pair (*AtFtsH3* and *AtFtsH10* in Arabidopsis, *OsFtsH3* and *OsFtsH8* in rice). The products of the other three Arabidopsis gene pairs are represented by single genes in rice. A unique feature of the organization of the *OsFtsH* gene family is that *OsFtsH4* and *OsFtsH5* are tandemly arrayed on the genome, suggesting they arose by a duplication event; in Arabidopsis, a single locus (*AtFtsH4*) corresponds to these genes. Collectively, the data in Figure 6 suggest that there is a core complement of higher plant FtsH genes and that the emergence of this core predates the monocot/dicot divergence. However, elaborations on this core occurred during the subsequent course of evolution.

Comparison of the predicted gene structures of the nine *OsFtsH* genes from the annotated pseudomolecule sequences with the sequences of cDNAs and ESTs revealed that the TIGR annotations of intron-exon borders are largely correct, with only a few discrepancies (data not shown). However, a comparison of the structures of the rice and corresponding Arabidopsis genes reveals a striking conservation of intron-exon
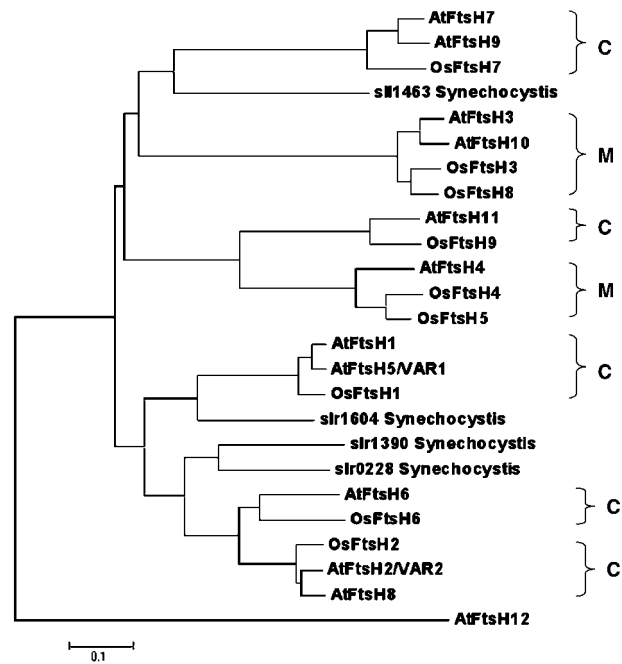

Figure 6. Conservation of *FtsH* genes in Arabidopsis and rice. Phylogenetic analysis of *FtsH* genes from Arabidopsis, rice, and Synechocystis. Full-length protein sequences were aligned using the ClustalW program, and the aligned sequences were analyzed by the Mega 2.1 program (Kumar et al., 2001; see also http://www.megasoftware.net). The neighbor-joining method was used to construct the phylogenetic tree.

borders and exon size. For instance, Figure 7 shows the structural conservation of the two sets of plastid-localized proteins in the upper and lower bands of the 2-D gels. This conservation is consistent with the idea that *FtsH* gene families in higher plants evolved from a common core of conserved enzymes.

Also consistent with the idea of a core are the results of comparative 2-D green gel analyses of thylakoid membranes isolated from rice (a monocot) and pea (*Pisum sativum*; like Arabidopsis, a dicot; Fig.

Table I. *Rice OsFtsH gene family*

The GenBank ID of each OsFtsH gene is shown. Also shown is its chromosomal and bacterial artificial chromosome (BAC) location on the rice genome (IRGSP BAC clone no.). Full-length protein sizes (amino acids) were obtained from TIGR pseudomolecule annotations and further checked against cDNA and EST sequences. Putative cellular locations were predicted using the TargetP program (Emanuelsson et al., 2000). The location of OsFtsH9 is problematic since it is predicted to be in the mitochondrion; however, its homolog in Arabidopsis (AtFtsH11) is in the chloroplast (Sakamoto et al., 2003). Partial or full-length cDNA sequences from GenBank (a representative ID no. is shown) are proof of expression. C, Chloroplast; M, mitochondrion; a.a., amino acid.

| Gene Name	Arabidopsis Homolog	GenBank ID	BAC Clone	Chromosome	Protein Size (a.a.)	Cellular Location	Expression
OsFtsH1	*AtFtsH1/5*	AP003685	P0548E04	6	686	C	AK065019
OsFtsH2	*AtFtsH2/8*	AP003635	P0686E06	6	676	C	AK064913
OsFtsH3	*AtFtsH3/10*	AP003240	P0406G08	1	802	M	AK100245
OsFtsH4	*AtFtsH4*	AP003413	B1151A10	1	709	M	AK072509
OsFtsH5	*AtFtsH4*	AP003413	B1151A10	1	715	M	AK120948
OsFtsH6	*AtFtsH6*	AP003569	P0425F05	6	681	C	AK063733
OsFtsH7	*AtFtsH7*	AP004868	P0048B08	2	822	C	AK069509
OsFtsH8	*AtFtsH3/10*	AC105770	OJ1362D02	5	822	M	AK069936
OsFtsH9	*AtFtsH11*	AP003328	B1040D09	1	769	C?	AK060394
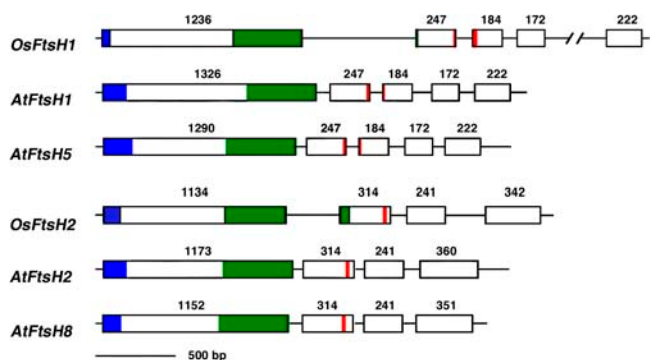
Figure 7. Structures of rice and Arabidopsis *FtsH* genes. Gene structures were constructed based on annotation of the Arabidopsis and rice genomes. Intron-exon boundaries were confirmed by examination of cDNA and EST sequences. Boxes indicate exons and lines represent introns. Numbers above each box refer to size of the exon (bp). Untranslated regions were not included in the structures. Colored regions correspond to various FtsH domains. Blue represents transit peptide region, green represents ATP-binding region, and red represents zinc-binding site.

2A). Similar to Arabidopsis, upper and lower FtsH-containing bands are present in both of these species (Fig. 8A). This was confirmed by western-immunoblot analyses of the 2-D gels using our AtFtsH1 and VAR2 antibodies, where bands corresponding to these proteins can be seen (Fig. 8B).

The western blots also reveal that streaking is apparent toward higher M_r areas of the 2-D gels of Arabidopsis thylakoid proteins when the VAR2 antibody is used as a probe. These results confirm earlier data and are consistent with the idea that VAR2 participates in oligomer formation (Yu et al., 2004). On the other hand, similar streaking is not seen using the AtFtsH1 antibody; we speculate this might be because of the low abundance of this protein and a consequent inability to detect oligomers. In a similar vein, the streaking is not detectable on the westerns in pea or rice using either antibody as a probe. This could mean that pea and rice do not form oligomers or that they are not abundant enough to be detected using Arabidopsis antibodies.

DISCUSSION

Subunit Interchangeability: Gene Duplication and Redundant Functions

E. coli has one *FtsH* gene, cyanobacteria have four (Kaneko et al., 1996), rice has at least nine (Table I), and Arabidopsis has 12 (Fig. 6). Why are so many *FtsH* genes needed in higher plants? These data show that a core complement of 7 FtsH genes was in place by the time of the monocot/dicot divergence (see Fig. 7). Some of these core genes subsequently became duplicated in Arabidopsis or rice. These include the genes in the upper and lower bands of the 2-D gels. One hypothesis is that the various FtsH proteins became

specialized in their activity. For instance, the chaperone activity of FtsH normally acts to promote the protease activity of the enzyme (Suzuki et al., 1997). However, it is possible the enzyme could act independently as a chaperone, as found in the Clp class of proteases (Nielsen et al., 1997). We found that members of the 2-8 and 1-5 duplicated pairs in Arabidopsis are interchangeable, while proteins of different pairs are not interchangeable. This lack of interchangeability does not necessarily mean that the members of the two pairs have different functions, e.g. it could simply signify an inability to assemble efficiently. Nevertheless, whether the two have similar, or different, functions is now under investigation.

Another hypothesis is that multicellularity required a subspecialization of function such that it became necessary for the various FtsH gene family members to differ in the timing and/or cell specificity of their expression. In this respect, it is interesting that all four *AtFtsH* genes (*AtFtsH1*, *2*, *5*, and *8*) have similar expression profiles, with abundant expression in green organs of the plant. Although our experiments were not refined enough to allow us to detect cell-specific differences in expression, the absolute levels of expression of these genes vary: *AtFtsH2* is the most highly expressed (at the mRNA and protein levels), followed by *AtFtsH1* and *AtFtsH5*, with approximately 50% of the mRNA and protein expression levels of *AtFtsH2*, and finally *AtFtsH8*, whose mRNA and protein expression are about 20% that of *AtFtsH2* (Sinvany-Villalobo et al., 2004). As Sinvany-Villalobo et al. (2004) have pointed out, these expression levels roughly correlate with the severity of phenotype observed in mutants that have lesions in these genes: Null mutants of *AtFtsH2* and *AtFtsH5* are variegated, whereas null (T-DNA insertion) mutants of *AtFtsH1* and *AtFtsH8* have no obvious phenotypic changes (Sakamoto et al., 2003; F. Yu and S. Rodermel, unpublished data).

Although we do not understand the reason for the quantitative differences in expression among the
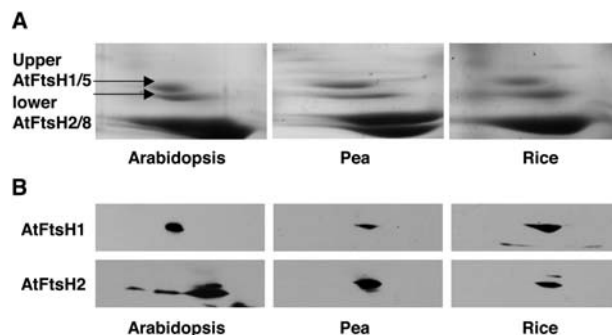

Figure 8. Comparative 2-D green gel analyses. A, 2-D green gels were prepared as described in Figure 2A using isolated thylakoid membranes from Arabidopsis, rice, and pea. The regions of each gel containing the upper and lower FtsH-containing bands are shown. B, Western immunoblots of 2-D gels probed with AtFtsH1 and VAR2 antibodies are shown.

various *AtFtsH* genes, our data indicate that chloroplast biogenesis requires AtFtsH complexes with two types of subunits (AtFtsH2 and 8) and (AtFtsH1 and 5). As discussed below, the attainment of threshold concentrations of these subunit types might be critical. If so, processes that promote this might have been important during evolution (e.g. increased gene copy number, increased expression levels). In this context, our data are reminiscent of Rubisco, where the large size of the nuclear Rubisco small subunit gene family has been attributed, in part, to the need to obtain high Rubisco concentrations in the chloroplast, rather than to a need for individual gene specialization (for review, see Rodermel, 1999). Consistent with this hypothesis is the observation that AtFtsH2 can form homo-oligmers, which might constitute a fraction of the AtFtsH complex pool (Sakamoto et al., 2003). This might not be unexpected because AtFtsH2 is the most abundant FtsH subunit. Regardless, how the total optimum AtFtsH pool size is attained is not known.

Mechanism of Variegation

The data in this study confirm and extend a model of variegation in which chloroplast function requires a threshold concentration of AtFtsH multimers (Yu et al., 2004). Below this threshold, a white plastid forms, while above this threshold, a normal chloroplast is produced. According to our revised model, AtFtsH complexes contain two types of subunits—AtFtsH2 and 8 and AtFtsH1 and 5. Because alterations in AtFtsH protein abundance do not influence *AtFtsH* transcript abundance, we propose that levels of the AtFtsH1 and 5 pair are matched with those of the AtFtsH2 and 8 pair, and that excess subunits are turned over. In cells in which the number of AtFtsH complexes is below the threshold, chloroplast differentiation is impaired, leading to the generation of white plastids. Conversely, plastids with threshold or higher levels of AtFtsH complex formation develop normal chloroplasts. We speculate that these decisions occur during the conversion of undifferentiated proplastids in the leaf meristem into mature chloroplasts early in leaf development. The process of sorting out of dividing plastids would then result in the generation of clones of white plastids and cells (white sectors) or clones of chloroplast-containing cells (green sectors).

If our model is correct, there are at least two possibilities to explain the threshold phenomenon. One is that there is unequal partitioning of a nuclear gene product to the plastids (>100) within a cell. For instance, in the case of *var1*, there could be unequal partitioning of AtFtsH1, with some plastids receiving more of this protein than others. An alternative explanation is that all plastids receive similar amounts of AtFtsH1, but that there might be intrinsic differences among plastids within a developing leaf cell in a biochemical process that is required for normal chloroplast development. For instance, there might be variability in rates of D1 repair, such that not all

plastids need the same amount of AtFtsH1 for this process to occur efficiently. Regardless of the precise mechanism, our model is in accord with early data showing that cells in the white sectors of *var2* are heteroplastidic and contain some normal-appearing chloroplasts, as well as a large number of abnormal plastids (Chen et al., 1999). This plastid autonomy indicates that not all plastids in a given cell are equivalent in function.

MATERIALS AND METHODS

Plant Material

Arabidopsis (*Arabidopsis thaliana* ecotype Columbia) and pea (*Pisum sativum*) were grown in growth rooms under continuous fluorescent lights (about 100 μmol m^{-2} s^{-1}) at 22°C. Rice (*Oryza sativa* sp. *japonica* cv Nipponbare) was grown in growth chambers under 16-h-day/8-h-night cycles at 28°C.

2-D Green Gel Analysis

Leaf tissues used in this study were collected from 3-week-old Arabidopsis plants, 3-week-old rice plants, and 2-week-old pea plants. Chloroplast membranes were isolated as previously described (Yu et al., 2004) by grinding the tissue in 0.33 M sorbitol, 10 mM EDTA, 50 mM HEPES, pH 8.0, and 0.05% bovine serum albumin using a Waring blender. The homogenate was filtered through two layers of Miracloth and centrifuged at 2,600g for 3 min. Crude chloroplasts were washed with 10 mM MOPS, pH 8.0, followed by centrifugation at 10,000g for 10 min. The pellet, which contains thylakoid membranes, was resuspended in 0.33 M sorbitol, 5 mM MgCl$_2$, and 50 mM HEPES, pH 8.0. Chlorophyll concentrations were measured on the resuspended membranes using 95% ethanol (Lichtenthaler, 1987). All the steps were performed at 4°C under dim light.

First-dimension green gel analysis was carried out as previously described (Yu et al., 2004). In brief, thylakoid membranes were solubilized in a mixture of detergents (0.45% octyl glucoside, 0.45% decyl maltoside, 0.1% lithium dodecyl sulfate, 10% glycerol, 2 mM Tris maleate, pH 7.0), and samples corresponding to 45 μg of chlorophyll were loaded onto a 3-mm 8% polyacrylamide (native) gel (MiniProtein II; Bio-Rad, Hercules, CA). The gels were electrophoresed at 4°C at 10 mA for 90 min. For the second dimension, gel strips were cut out of the native gels and incubated in 2 × SDS sample buffer (Laemmli, 1970) at 65°C for 2 h. SDS-PAGE was then performed as described using 14% SDS-polyacrylamide gels (Xu et al., 1994).

Antibody Production, Coimmunoprecipitation, and Western Immunoblotting

To generate a specific antibody for AtFtsH1, a 15-amino acid peptide PLFIQNEILKAPSPK that is specific for AtFtsH1 was synthesized, and polyclonal antibodies were generated in rabbits (ProSci, Poway, CA). The antibody was used at a 1:10,000 dilution.

Nucleotide fragments corresponding to amino acids P196-G353, A51-S229, and G367-V507 of the D1 protein of PSII, the cytochrome b_6f Rieske protein (PetC), and the ATP synthase α-subunit, respectively, were amplified by PCR and subcloned into the pET15b vector (Novagen, Madison, WI). The resulting constructs were transferred and expressed in *Escherichia coli* BL21(DE3) (Novagen). All the expressed peptides formed inclusion bodies, which were purified and solubilized (by procedures suggested by the manufacturer) and injected into rabbits. After three injections, cleared sera were used as antibodies against each antigen. All three antibodies were used at a 1:1,000 dilution.

Coimmunoprecipitations were carried out essentially as described by Sakamoto et al. (2003). Briefly, thylakoid membranes were suspended in phosphate-buffered saline at a concentration of 0.8 mg chlorophyll/mL, then solubilized with 0.8% dodecylmaltoside. After 30-min incubation on ice, samples were diluted to 0.1 mg chlorophyll/mL and antibodies against AtFtsH1 or AtFtsH2/VAR2 were added. Sepharose-coupled protein A was

added after 4 h and the samples were incubated overnight at 4°C. Immuno-precipitates were recovered by centrifugation at 12,000g for 15 s, then washed three times with phosphate-buffered saline containing 0.05% dodecylmalto-side. Finally, the samples were boiled for 5 min in 2× SDS buffer and subjected to standard SDS-PAGE.

For western immunoblotting, proteins were transferred from 12% SDS-polyacrylamide gels to nitrocellulose membranes (Immobilon-NC; Millipore, Billerica, MA) and probed with various antibodies. The AtFtsH2/VAR2 antibody was described in Chen et al. (2000); it detects both AtFtsH2 and 8. The SuperSignal West Pico chemiluminescence kit (Pierce, Rockford, IL) was used for signal detection. The nitrocellulose membranes were stained after transfer with Ponceau S to examine loading efficiency and transfer quality.

Plasmid Construction and Arabidopsis Transformation

To generate an *AtFtsH1* overexpression construct, an *AtFtsH1* cDNA was amplified using *pfx* DNA polymerase (Invitrogen, Carlsbad, CA) with forward primer 5′-AACCTCGAGACGAAGAAGAAGAAACAGAGCTGC-3′ and reverse primer 5′-AACCTCGAGTGTAAGCACTAAGCAATGGCA-ACT-3′ (*Xho*I sites underlined). The PCR product was digested with *Xho*I and cloned into the *Xho*I site of pBlueScript. The resulting plasmid was sequenced for errors. The *AtFtsH1* cDNA fragment was isolated and cloned into the *Xho*I site of a binary vector derived from pBI121 (Yu et al., 2004). This vector lacks the GUS gene, but contains the CaMV 35S promoter and the *NPTII* (*neomycin phosphotransferase*) gene separated by a multiple cloning site. The resultant plasmid was named pBI111LF1C. To generate *var1-1* plants that overexpress *AtFtsH1*, pBI111LF1C was mobilized into *Agrobacterium tumefaciens* and *var1-1* plants were transformed by the *A. tumefaciens*-mediated floral-dip method (Clough and Bent, 1998). Kanamycin-resistant plants were selected at the T1 generation on plates containing 1× Murashige and Skoog salts, 1% Suc, 0.8% agar (pH 5.7) supplemented with 50 μg/mL kanamycin. PCR and Southern blotting were performed to verify that the plants were transformed. Segregation of phenotypes was scored in the T2 generation; RNA and protein analyses were also performed using T2 generation plants.

To generate an *AtFtsH1* antisense construct, a 1,500-bp *AtFtsH1* cDNA fragment from pBI111LF1C was cut out using *Xho*I and *Sst*I and then inserted into a pBI111L plasmid digested with *Xho*I and *Sst*I. In this way, this *AtFtsH1* cDNA fragment is under 35S promoter control in antisense orientation.

To generate an *AtFtsH2/VAR2* overexpression construct, forward primer 5′-ATAGGATCCAGATTCTCCTTCCCTATACAACTCT-3′ and reverse primer 5′-ATAGGATCCGAGATAGTATCACATTTCTAGAGTG-3′ (*Bam*HI site underlined) were used to amplify *AtFtsH2/VAR2* full-length cDNA. The cloning procedure is essentially the same as the *AtFtsH1* construct above, except the restriction enzyme used is *Bam*HI.

To generate *AtFtsH1* and AtFtsH5/VAR1 promoter-GUS fusion constructs, a similar approach was taken as in Yu et al. (2004). The primers for *AtFtsH1* are forward primer 5′-CATTCTAGAAGCTCTCACTGTTGTGTTACTCTT-3′ and reverse primer 5′-CATTCTAGATACTTGCGACGAGAATGGCGAATT-3′ (*Xba*I site underlined). The primers for *AtFtsH5/VAR1* are forward primer 5′-CATGGATCCCAACATCTATGTACTAGAATCTAG-3′ and reverse primer 5′-CATGGATCCGAACAACAGAGCTGCTAACGCAGC-3′ (*Bam*HI site underlined).

Manipulations of DNA and RNA

Genomic DNAs were isolated and Southern-blot analyses were performed as described in Wetzel et al. (1994). Total cell RNAs were isolated from plants using the Trizol RNA Reagent (Invitrogen). Semiquantitative RT-PCR was carried out essentially as described in Yu et al. (2004). In brief, the RNA was reverse transcribed using the SuperScript first-strand synthesis system for RT-PCR (Invitrogen). The RT reaction products were diluted 10 times, and the PCR reactions were performed using 32 cycles in a total volume of 50 μL. This is within the linear range of amplification for each of the fragments examined. Gene-specific primers for *AtFtsH1* were 5′-GTCTCAAGACGAAAATTCGC-3′ and 5′-GCCTGAAAAGCAAGAAGAGT-3′. Gene-specific primers for *AtFtsH2/VAR2* were 5′-ACTCTCATCTGTAATCGATA-3′ and 5′-ACCAAT-CAAGTTGAATAACAC-3′. Gene-specific primers for *AtFtsH5/VAR1* were 5′-CAACCACCAGCACCAACCAT-3′ and 5′-CTCTAAAGAGATAAAACA-ACC-3′. Gene-specific primers for *AtFtsH8* were 5′-TCTTCTGCCAAATTC-CACAG-3′ and 5′-CCCAATCAAGTTGAGTATTGG-3′. Gene-specific primers for the *Actin 2* gene were 5′-TCAAAGACCAGCTCTTCCATCGAGA-3′ and 5′-ACACACAAGTGCATCATAGAAACGA-3′.

LITERATURE CITED

Bailey S, Thompson E, Nixon PJ, Horton P, Mullineaux CW, Robinson C, Mann NH (2002) A critical role for the Var2 FtsH homologue of *Arabidopsis thaliana* in the photosystem II repair cycle in vivo. J Biol Chem **277:** 2006–2011

Beyer A (1997) Sequence analysis of the AAA protein family. Protein Sci **6:** 2043–2058

Chen M, Choi Y, Voytas DF, Rodermel SR (2000) Mutations in the Arabidopsis *VAR2* locus cause leaf variegation due to the loss of a chloroplast FtsH protease. Plant J **22:** 303–313

Chen M, Jensen M, Rodermel SR (1999) The *yellow variegated* mutant of *Arabidopsis* is plastid autonomous and delayed in chloroplast biogenesis. J Hered **90:** 207–214

Clough SJ, Bent AF (1998) Floral dip: a simplified method for *Agrobacterium*-mediated transformation of *Arabidopsis thaliana.* Plant J **16:** 735–743

Emanuelsson O, Nielsen H, Brunak S, von Heijne G (2000) Predicting subcellular localization of proteins based on their N-terminal amino acid sequence. J Mol Biol **300:** 1005–1016

Goff SA, Ricke D, Lan TH, Presting G, Wang R, Dunn M, Glazebrook J, Sessions A, Oeller P, Varma H, et al (2002) A draft sequence of the rice genome (*Oryza sativa* L. ssp. *Japonica*). Science **296:** 92–100

Hugueney P, Bouvier F, Badillo A, D'Harlingue A, Kuntz M, Camara B (1995) Identification of a plastid protein involved in vesicle fusion and/or membrane protein translocation. Proc Natl Acad Sci USA **92:** 5630–5634

Kaneko T, Sato S, Kotani H, Tanaka A, Asamizu E, Nakamura Y, Miyajima N, Hirosawa M, Sugiura M, Sasamoto S, et al (1996) Sequence analysis of the genome of the unicellular cyanobacterium *Synechocystis* sp. strain PCC6803. II. Sequence determination of the entire genome and assignment of potential protein-coding regions. DNA Res **3:** 109–136

Kumar S, Tamura K, Jakobsen IB, Nei M (2001) MEGA2: Molecular Evolutionary Genetics Analysis Software. Arizona State University, Tempe, AZ

Laemmli UK (1970) Cleavage of structural proteins during the assembly of the head of bacteriophage T4. Nature **277:** 680–685

Lichtenthaler HK (1987) Chlorophylls and carotenoids: pigments of photosynthetic biomembranes. Methods Enzymol **148:** 350–382

Lindahl M, Spetea C, Hundal T, Oppenheim AB, Adam Z, Andersson B (2000) The thylakoid FtsH protease plays a role in the light-induced turnover of the photosystem II D1 protein. Plant Cell **12:** 419–431

Lindahl M, Tabak S, Cseke L, Pichersky E, Andersson B, Adam Z (1996) Identification, characterization, and molecular cloning of a homologue of the bacterial FtsH protease in chloroplasts of higher plants. J Biol Chem **271:** 29329–29334

Martínez-Zapater JM (1993) Genetic analysis of variegated mutants in *Arabidopsis.* J Hered **84:** 138–140

Nielsen E, Akita M, Davila-Aponte J, Keegstra K (1997) Stable association of chloroplastic precursors with protein translocation complexes that contain proteins from both envelope membranes and a stromal Hsp100 molecular chaperone. EMBO J **16:** 935–946

Ostersetzer O, Adam Z (1997) Light-stimulated degradation of an un-assembled Rieske FeS protein by a thylakoid-bound protease: the possible role of the FtsH protease. Plant Cell **9:** 957–965

Rodermel S (1999) Subunit control of Rubisco biosynthesis—a relic of an endosymbiotic past? Photosynth Res **59:** 105–123

Rodermel S (2001) *Arabidopsis* variegation mutants. *In* CR Somerville, EM Meyerowitz, eds, The Arabidopsis Book. American Society of Plant Biologists, Rockville, MD (http://www.aspb.org/publications/arabidopsis)

Sakamoto W, Tamura T, Hanba-Tomita Y, Sodmergen, Murata M (2002) The *VAR1* locus of *Arabidopsis* encodes a chloroplastic FtsH and is

responsible for leaf variegation in the mutant alleles. Genes to Cells **7:** 769–780

Sakamoto W, Zaltsman A, Adam Z, Takahashi Y (2003) Coordinated regulation and complex formation of *yellow variegated 1* and *yellow variegated 2*, chloroplastic FtsH metalloproteases involved in the repair cycle of photosystem II in Arabidopsis thylakoid membranes. Plant Cell **15:** 2843–2855

Sinvany-Villalobo G, Davydov O, Ben-Ari G, Zaltsman A, Raskind A, Adam Z (2004) Expression in multigene families. Analysis of chloroplast and mitochondrial proteases. Plant Physiol **135:** 1336–1345

Suzuki CK, Rep M, van Dijl JM, Suda K, Grivell LA, Schatz G (1997) ATP-dependent proteases that also chaperone protein biogenesis. Trends Biochem Sci **22:** 118–123

Takechi K, Sodmergen, Murata M, Motoyoshi F, Sakamoto W (2000) The *YELLOW VARIEGATED (VAR2)* locus encodes a homologue of FtsH, an ATP-dependent protease in Arabidopsis. Plant Cell Physiol **41:** 1334–1346

Vision TJ, Brown DG, Tanksley SD (2000) The origins of genomic duplications in Arabidopsis. Science **290:** 2114–2117

Wetzel CM, Jiang CZ, Meehan LJ, Voytas DF, Rodermel SR (1994) Nuclear-organelle interactions: the *immutans* variegation mutant of *Arabidopsis* is plastid autonomous and impaired in carotenoid biosynthesis. Plant J **6:** 161–171

Xu Q, Jung YS, Chitnis VP, Guikema JA, Golbeck JH, Chitnis PR (1994) Mutational analysis of photosystem I polypeptides in *Synechocystis* sp. PCC 6803. Subunit requirements for reduction of NADP+ mediated by ferredoxin and flavodoxin. J Biol Chem **269:** 21512–21518

Yu F, Park S, Rodermel SR (2004) The Arabidopsis FtsH metalloprotease gene family: interchangeability of subunits in chloroplast oligomeric complexes. Plant J **37:** 864–876

Yu J, Hu S, Wang J, Wong GK, Li S, Liu B, Deng Y, Dai L, Zhou Y, Zhang X, et al (2002) A draft sequence of the rice genome (*Oryza sativa* L. spp. *Indica*). Science **296:** 79–92